IEEE Access
Multidisciplinary : Rapid Review : Open Access Journal

Received November 27, 2019, accepted January 22, 2020, date of publication February 3, 2020, date of current version February 12, 2020.

Digital Object Identifier 10.1109/ACCESS.2020.2971028

Design of Wideband Bandpass Filter With Simultaneous Bandwidth and Notch Tuning Based on Dual Cross-Shaped Resonator

CHENG TENG[1], (Student Member, IEEE), PEDRO CHEONG[1,2], (Member, IEEE), SUT-KAM HO[1], KAM-WENG TAM[1], (Senior Member, IEEE), AND WAI-WA CHOI[1], (Senior Member, IEEE)

[1]Faculty of Science and Technology, University of Macau, Macau 999078, China
[2]Poly-Grames Research Center, Department of Electrical Engineering, Ecole Polytechnique de Montreal, Montreal, QC H3T 1J4, Canada

Corresponding author: Cheng Teng (419805558@qq.com)

This work was supported in part by the Macao Science and Technology Development Fund under Grant FDCT 014/2015/AMJ, and in part by the University of Macau Research Projects under Grant MYRG 2018-00076-FST.

ABSTRACT In this paper, a wideband bandpass filter (BPF) with simultaneous bandwidth and notch tuning is proposed, by using a dual cross-shaped resonator (DCSR) with parallel-coupled three-line (PCTL) feeding. It is found that three intrinsic transmission zeros can be generated by the proposed DCSR, while two of the zeros are used for the implementation of passband edge zeros and the other one is for a notch. Three varactors are used to implement the bandwidth and notch tuning independently. These innovative integrated functions of both tunable bandwidth and notch in a single architecture are proposed for the first time. On the other hand, the PCTL can provide sufficiently strong coupling in the desired passband. The proposed BPF can achieve the bandwidth tuning with a fixed notch inside/outside the passband, and the bandwidth can also be kept unchanged when tuning a notch within the passband. The prototyped BPF centered at 6 GHz reports that the absolute bandwidth (ABW) can be varied from 2.5 to 5.8 GHz, while the fractional bandwidth (FBW) is tuned from 41.7% to 96.7% together with notch frequency tuning of 5.0 to 8.2 GHz. The experimental measurements are in good agreement with the theoretical analysis.

INDEX TERMS Microstrip wideband bandpass filters, dual cross-shaped resonator (DCSR), bandwidth and notch tuning, tunable filters.

I. INTRODUCTION

In various wireless communication and radar systems with multi-function and multi-band operations, the bandpass filters (BPFs) with reconfigurable center frequency and bandwidth are essential. To avoid interference from other systems, BPFs with notch bands are becoming more significant than the past. The primary efforts of previous studies mainly focus on center frequency tuning. By varying the electrical lengths of the resonators, the center frequency can be tuned continuously either with the use of varactors [1]–[3] or reconfigured in discrete steps by using PIN diodes [4], [5]. For example, the filter's center frequency is tuned from 0.7 to 1.33 GHz with a 60% tuning range using varactors as the tuning elements [1]; while a six-state reconfigurable bandpass filter with center frequency to be 9, 10 and 11 GHz using PIN diodes [4].

Nevertheless, the BPFs with reconfigurable bandwidth are still rare, especially for wideband BPFs. Some approaches were proposed in [6]–[8], varactors or PIN diodes are used for connecting tuning stubs or open loops. A three-pole microstrip BPF with a tunable bandwidth of 70 – 100 MHz is presented in [6], by using only one varactor between the resonators for bandwidth control. Another BPF uses a single PIN diode as a switch to connect or disconnect the loaded open-loop and reported the bandwidth tuned from 29% to 50% at 1.5 GHz [7]. But this design can only achieve two tuning states. A tunable wideband BPF controlled by switching short circuit stubs can achieve the bandwidth range from 16.3% to 37.4% at 2 GHz with four tuning states [8], but the passband edge selectivity is concerned. A tunable bandpass filter with continuous control of both center frequency and

The associate editor coordinating the review of this manuscript and approving it for publication was Vincenzo Conti.

bandwidth is presented in [9], which indicates wide tunable center frequencies (0.56 – 1.15 GHz) and 1-dB bandwidth (65 – 180 MHz), it is still applied for the narrow band.

In addition to reconfigurable bandwidth, wideband filters with notch bands are important for their applications of interference rejection. The techniques for fixed notch bands design using additional notch resonators and embedded open stubs are presented in [10]–[12]. Nowadays, there is an increasing demand for reconfigurable notch bands to cope with different coexisted communication. A switchable notch filter employing 1-D planar EBG is demonstrated in [13], the frequency of the notch band can be switched by 450 MHz.

Recently, the multi-mode resonator (MMR) is used to design wideband and ultra-wideband (UWB) BPFs [14]–[16]. A ring resonator BPF with switchable bandwidth using multiple open stubs was proposed, the tunable passband ratio is 1.22: 1.13: 1 at 2.45 GHz [17]. A simple MMR called cross-shaped resonator (CSR) is presented, which can generate distinct numbers of poles and zeros with different terminations. We have also reported some studies based on the CSR [18]–[21]. A four poles filter is shown in [18], with 82.4% FBW and reconfigurable notch from 4.6 to 6.5 GHz are designed, by using capacitors as the tuning elements. Besides, two wideband tunable BPFs based on CSR tuned by varactors with FBW tuning of 50.4% and 83% respectively at 1.0 GHz, are reported in [19]. In addition, a wideband BPF with reconfigurable bandwidth using CSR with FBW tuning of 21.7% at 5.7 GHz, is proposed in [20], PIN diodes are used as the tuning elements. Another PIN diode tuned dual-band BPF with a reconfigurable lower passband edge is achieved [21], with 22.5% to 34.7% FBW tuning for the first passband. However, although the previous studies can achieve the reconfigurable bandwidth and notch individually, there are no existing designs that can accommodate both bandwidth and notch tuning simultaneously in a single structure.

In this work, the objective is to achieve the bandwidth and notch tuning in a single BPF. To this end, a dual cross-shaped resonator (DCSR) is presented, and the relationship between the poles/zeros and the other parameters are analyzed. The proposed BPF is fabricated on a RO4003 substrate with a thickness of 0.813 mm and a dielectric constant of 3.38. Simulations are carried out by Ansys HFSS. The varactors, Toshiba JDV2S71E with a capacitance tuning range of 0.6 – 6.0 pF; and the capacitors, Murata GRM series (CAP CER 50V C0G/NP0 0603) for 1.2 pF and 4.0 pF with ±0.1 pF tolerance, are used to achieve the different electrical tunable functions.

This paper is organized as follows. Besides the introductory section, a tunable wideband BPF using DCSR with PCTL is thus presented. The structure will be analyzed in Section II; and then in section III, the method of varactors to achieve the simultaneous bandwidth and notch tuning is presented; a prototype with simulated and measured results is shown in Section IV, and a comparison with previous works are summarized. Finally, the conclusion is summarized in Section V.

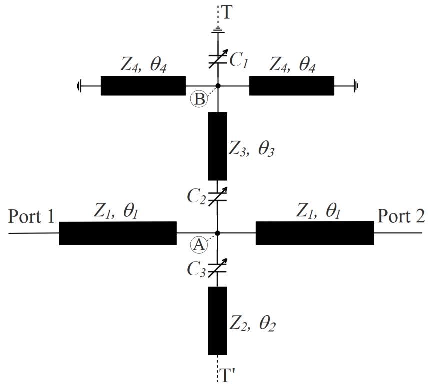

FIGURE 1. Schematic of the proposed DCSR.

II. ANALYSIS OF THE DCSR AND PCTL

A. DUAL CROSS-SHAPED RESONATOR (DCSR)

The schematic of the proposed DCSR is shown in Fig. 1. The parameters θ_n and Z_n ($n = 1, 2, 3, 4$) denote the electrical lengths and characteristic impedances of these stubs, respectively. We also define Y_n as the admittances of stubs. A terminated cross-shaped branch consists of two shorted stubs (Z_4, θ_4) and a terminated varactor with variable capacitive (C_1), is added to a transmission line (Z_3, θ_3). On the other hand, a varactor (C_2) is connected between the central resonator (Z_1, θ_1) and stub (Z_3, θ_3); besides, an open stub (Z_2, θ_2) is also added to the central resonator with another connecting varactor (C_3). In addition, we set the upper cross center as Ⓐ, and the lower one as Ⓑ.

To ease the discussion, a BPF with 100% FWB, 6 GHz as center frequency and a fixed notch at 7 GHz are to be designed with 100 Ω for Z_1, with a fixed capacitance of 1.0 pF for C_1, C_2, and C_3. Meanwhile, we assume that $k_1 = Z_1/Z_2 = Z_1/Z_3$ and $k_2 = Z_1/Z_4$. In this case, the proposed DCSR is symmetrical to the T-T' plane, and its odd- and even-mode equivalent circuits are shown in Fig. 2, respectively. Based on these equivalent circuits, the input admittance of these two modes can be derived as follows:

For odd mode:

$$Y_{ino} = \frac{1}{jZ_1 \tan\theta_1} \tag{1}$$

The odd mode resonant frequency is determined when $Y_{ino} = 0$. Therefore, $\theta_1 = 90°$, which represents that a transmission pole is at the center frequency f_0.

For even mode:

$$Y_{ine} = \frac{Y_1 (Y_r + jY_1 \tan\theta_1)}{Y_1 + jY_r \tan\theta_1} \tag{2a}$$

where

$$Y_r = Y_u + Y_d \tag{2b}$$

$$Y_d = \frac{j\omega C_3 Y_2 \tan\theta_2}{\omega C_3 + 2Y_2 \tan\theta_2} \tag{2c}$$

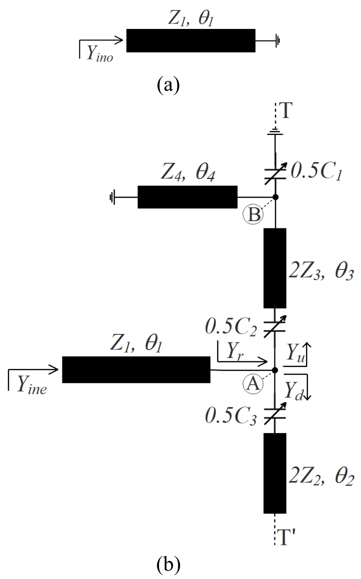

FIGURE 2. (a) Odd- and (b) even-mode equivalent circuits of the proposed DCSR.

And Y_u and Y_d are the input admittances of the upper and lower resonator branches respectively. Thus, they can be expressed by (2c) and as (2d) shown at the bottom of this page. Similar to the previous case, the transmission poles can be determined with $Y_{ine} = 0$. Therefore, the even mode resonant frequencies can be expressed by (3a), (3b), and (3c) as shown at the bottom of this page, where c is the speed of light in free space, ε_r denotes the effective dielectric constant and l_n ($n = 1, 2, 3, 4$) stands for the physical lengths of the stubs.

The transmission coefficient S_{21} can be expressed as:

$$S_{21} = \frac{Y_{ino} - Y_{ine}}{(Y_0 + Y_{ino})(Y_0 + Y_{ine})} \tag{4}$$

The transmission zeros are thus determined when $S_{21} = 0$ and hence $Y_{ino} = Y_{ine}$. The transmission zeros in terms of C_1, C_2, and C_3 can be expressed as:

$$f_{notch} = \frac{c}{2\pi l_4\sqrt{\varepsilon_r}} \cot^{-1}\left(\frac{\omega C_1 Z_1^2}{k_1 k_2}\right) \tag{5a}$$

$$f_{z1} = \frac{c}{2\pi l_3\sqrt{\varepsilon_r}} \cot^{-1}\left(\frac{k_1^2}{\omega C_2 Z_1^2 - \Delta}\right) \tag{5b}$$

$$f_{z2} = \frac{c}{2\pi l_2\sqrt{\varepsilon_r}} \cot^{-1}\left(\frac{k_1^2}{\omega C_3 Z_1^2}\right) \tag{5c}$$

where

$$\Delta = \frac{k_1 k_2 Z_1 \tan\left(\frac{2\pi l_4\sqrt{\varepsilon_r}}{c} f_{z1}\right)}{k_1 - 2\pi f_{z1} Z_1^2 C_1 \tan\left(\frac{2\pi l_4\sqrt{\varepsilon_r}}{c} f_{z1}\right)} \tag{5d}$$

According to the analysis above, it can be seen that this DCSR can generate four transmission poles ($f_{p1}, f_{p2}, f_0, f_{p3}$) and three zeros ($f_{z1}, f_{notch}, f_{z2}$), which can be controlled by the capacitor C_1, C_2, and C_3. To form the passband and an in-band notch frequency, the following condition should be satisfied:

$$f_{z1} < f_{p1} < f_0 < f_{p3} < f_{z2} \tag{6a}$$

$$f_{p1} < f_{p2} < f_{p3} \text{ and } f_{z1} < f_{notch} < f_{z2} \tag{6b}$$

The variables Z_2, Z_3, Z_4, θ_2, θ_3, and θ_4 can be determined according to the characteristics of the BPF. Fig. 3(a) plots the transmission poles and zeros frequencies against θ_2/θ_1 under different values of k_1 when $k_2 = 1$ and $\theta_3/\theta_1 = \theta_4/\theta_1 = 1$. It can be noticed that the variations of both θ_2/θ_1 and k_1 affect the upper passband edge. f_{z2} and f_{p3} move closer to the center frequency f_0 for larger θ_2/θ_1 or larger k_1, while the other poles and zeros are almost unchanged. According to the FBW, the cutoff frequency of the upper passband edge is designed around 9 GHz, θ_2 is thus chosen to be 60°. The variations of poles and zeros versus θ_3/θ_1 under different values of k_1 when $k_2 = 1$, $\theta_2 = 60°$, and $\theta_4/\theta_1 = 1$, is illustrated in Fig. 3(b). It shows that f_{notch} moves from higher to lower frequency when θ_3/θ_1 increases. $\theta_3 = 40°$ is thus selected according to the notch frequency we want to design at. In addition, combine Fig. 3(a) and 3(b), the upper passband edge is good at about $k_1 = 1$. Fig. 3(c) studies

$$Y_u = \frac{j\omega C_2 Y_3 (\omega C_1 + Y_3 \tan\theta_3 - 4Y_4 \cot\theta_4)}{2\omega Y_3 (C_1 + C_2) + 2\omega C_2 \tan\theta_3 (2Y_4 \cot\theta_4 - \omega C_1) + 4Y_3 (Y_3 \tan\theta_3 - Y_4 \cot\theta_4)} \tag{2d}$$

$$f_{p1} = \frac{c}{2\pi (l_1 + l_3 + l_4)\sqrt{\varepsilon_r}} \tan^{-1}\left(\frac{\frac{2}{\omega Z_1} - \omega C_1 C_2 k_1 k_2}{C_1 k_2 - C_2 k_1}\right) \tag{3a}$$

$$f_{p2} = \frac{c}{2\pi (l_1 + l_3 + l_4)\sqrt{\varepsilon_r}} \tan^{-1}\left(\frac{\frac{2}{\omega Z_1} + \omega C_1 C_2 k_1 k_2}{C_1 k_2 - C_2 k_1}\right) \tag{3b}$$

$$f_{p3} = \frac{c}{2\pi (l_1 + l_2)\sqrt{\varepsilon_r}} \tan^{-1}\left(\frac{2}{2 - \omega C_3 Z_1 k_1}\right) \tag{3c}$$

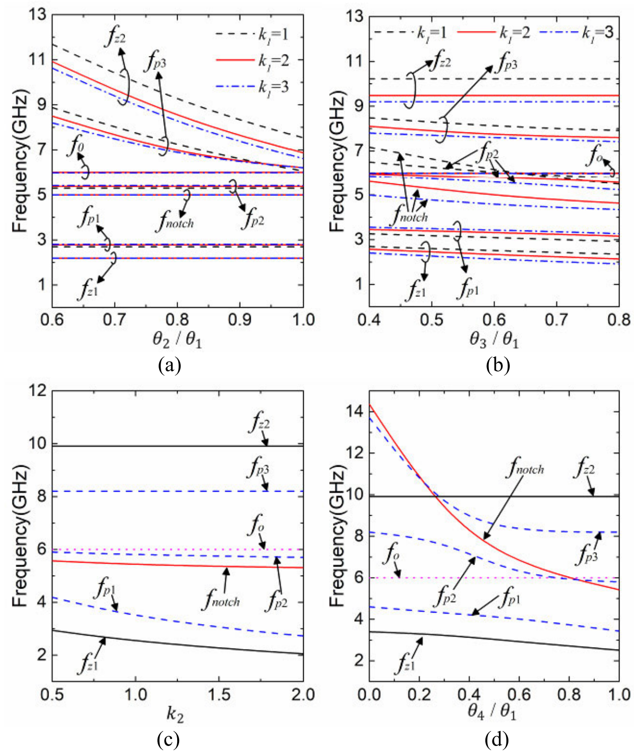

FIGURE 3. Variation of the poles and zeros versus (a) varied θ_3/θ_1 when $k_2 = 1$ and $\theta_2/\theta_1 = \theta_4/\theta_1 = 1$; (b) varied θ_2/θ_1 when $k_2 = 1$, $\theta_3 = 60°$ and $\theta_4/\theta_1 = 1$; (c) varied k_2 when $\theta_3 = 60°$, $\theta_2 = 40°$ and $k_1 = 2$; and (d) varied θ_4/θ_1 when $\theta_3 = 60°$, $\theta_2 = 40°$, $k_1 = 2$ and $k_2 = 1$.

the variation of poles and zeros versus k_2 when $\theta_2 = 60°$, $\theta_3 = 40°$, $k_1 = 1$, and $\theta_4/\theta_1 = 1$. The lower passband edge frequencies f_{z1} and f_{p1} depart from the center frequency for larger k_2. Therefore, k_2 is chosen to be 1.5 when the lower passband edge cut off frequency is designed as about 3 GHz. The relationship between poles and zeros and θ_4/θ_1 when is studied in Fig. 3(d). For a lower θ_4/θ_1, f_{notch} moves from lower to a higher frequency, and it will be out of the upper passband edge ($f_{notch} > f_{z2}$) when θ_4/θ_1 is lower than 0.3 since the notch frequency is designed at 7 GHz, θ_4/θ_1 is therefore decided to be 0.5.

Based on above, the following dimensions and relevant parameters are used: $Z_1 = 100\ \Omega$, $k_1 = 1$, $k_2 = 1.5$, $Z_2 = Z_3 = 100\ \Omega$, $Z_4 = 67\ \Omega$, $\theta_1 = 90°$, $\theta_2 = 60°$, $\theta_3 = 40°$, $\theta_4 = 45°$, $C_1 = 1.0$ pF, $C_2 = 1.0$ pF, and $C_3 = 1.0$ pF. The simulated frequency response of this DCSR is shown in Fig. 4.

B. PARALLEL COUPLED THREE-LINES (PCTL)

To incorporate the DCSR for a wideband BPF with tunable functions, the central open stub of DCSR is replaced by the PCTL [16], [22], [24] which can provide a tight coupling. The layout of the proposed tunable BPF is shown in Fig. 5. The relationship between the line width w_1, gap size s of the PCTL and the loaded quality factor are studied in [18]. Specifically, $w_1 = s = 0.1$ mm is determined to satisfy the characteristics of the BPF we want to design. The simulated

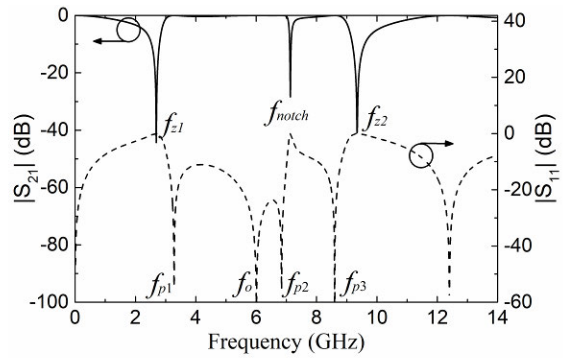

FIGURE 4. Simulated frequency response of the DCSR.

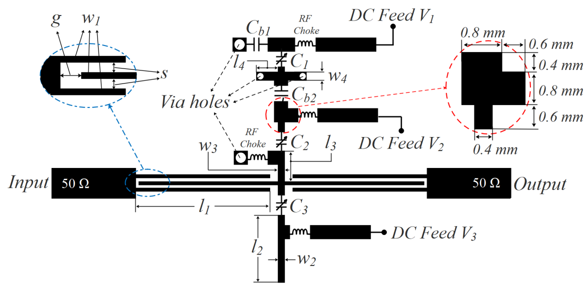

FIGURE 5. Layout of the proposed tunable BPF.

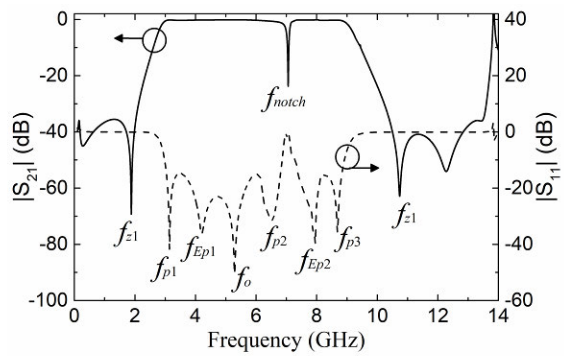

FIGURE 6. Simulated frequency response of the DCSR fed by the PCTL.

frequency responses of DCSR fed by the PCTL is shown in Fig. 6. Compared with Fig. 4 and Fig. 6, it can be seen that two extra poles (f_{Ep1}, f_{Ep2}) in the designed passband and two extra transmission zeros will be generated outside the passband, resulting in wide upper and lower stopbands.

III. TUNABLE BPF DESIGN

The tunability of the proposed BPF can be determined by the varactors. Three different DC voltage will be applied on the BPF, and the variable capacitance C_1, C_2, and C_3 can be controlled by suitable voltages V_1, V_2 and V_3. Fig. 7(a) shows the variation of pols and zeros when C_3 is variable and C_1 and C_2 are fixed on 1.0 pF. It can be seen that for a larger C_3, only f_{z2} and f_{p3} lower to the center frequency, while the others are unchanged. Fig. 7(b) plots the relationship between poles, zeros and the capacitance C_2 when C_1 and C_3 are fixed on

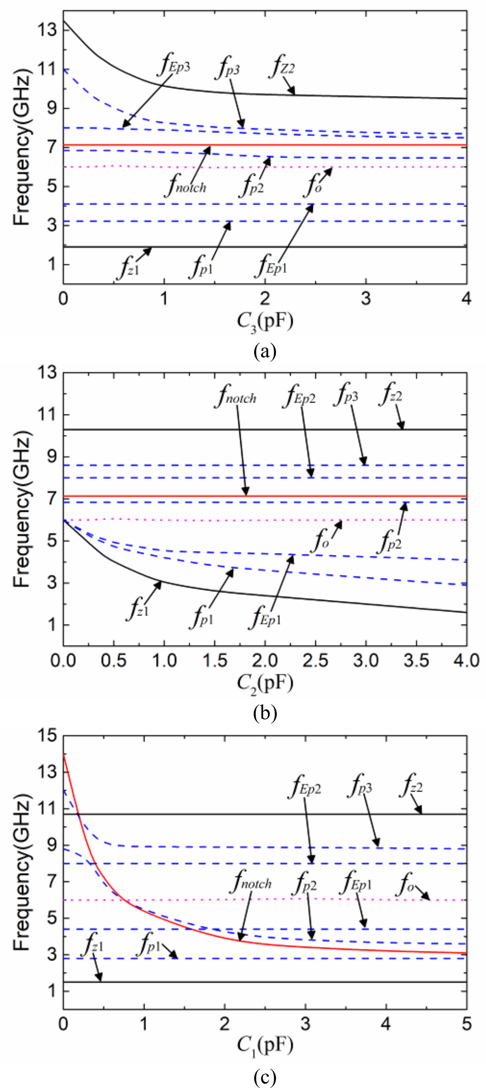

FIGURE 7. Variation of the poles and zeros versus (a) varied C_3 when $C_1 = C_2 = 1.0$ pF; (b) varied C_2 when $C_1 = 1$ pF, $C_3 = 0.5$ pF and (c) varied C_1 when $C_2 = 4.0$ pF, $C_3 = 0.5$ pF.

1.0 and 0.5 pF. When C_2 decreases from 4.0 to 0 pF, $f_{z2,}$ and f_{p1} move closer to the center frequency, while the other poles and zeros are constant. Besides, the relationship between poles, zeros and capacitance C_1 is shown in Fig. 7(c), C_2, C_3 are fixed as 4.0 pF and 0.5 pF respectively. It can be seen that when C_1 is within 0.3 to 5.0 pF, f_{notch} and f_{p2} moves to a higher frequency with a lower value of C_1, while the other poles and zeros frequencies are kept unchanged. However, when $C_1 < 0.3$ pF, f_{notch} will be out of the passband.

Accordingly, it is apparent that f_{notch} and f_{p2} can be controlled by C_1, while (f_{z1}, f_{p1}) and (f_{z2}, f_{p2}) can be varied by C_2 and C_3 respectively, which are in agreement with (3a), (3b), (3c) and (5a), (5b), (5c). Therefore, the intrinsic zero f_{notch} can be used to implement a tunable notch frequency, and it can also be designed in/out of the passband according to the capacitance C_1. (f_{z1}, f_{p1}) and (f_{z2}, f_{p2}) can be used to design as the lower and upper cutoff frequencies of the passband edges respectively. That is to say, the bandwidth tuning can be approximated to the poles and zeros tuning by varactors C_2 and C_3.

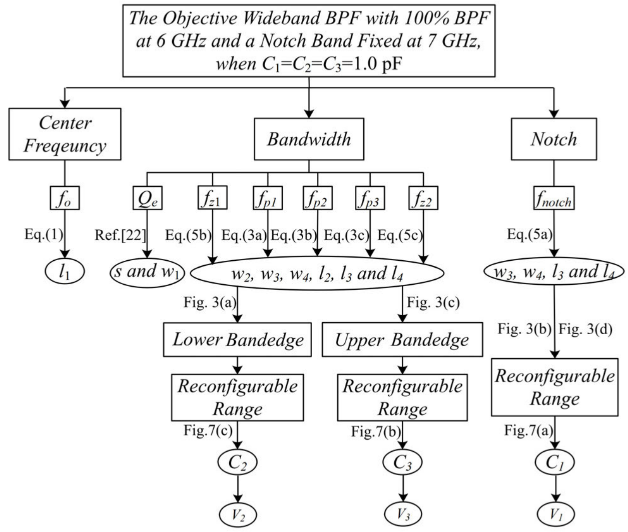

FIGURE 8. Design procedure of the proposed tunable BPF.

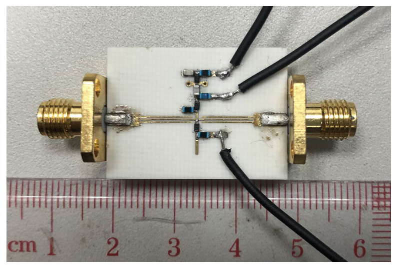

FIGURE 9. Prototype of the proposed tunable BPF.

The filter design procedure is summarized as a flowchart, as shown in Fig. 8:

1) When the desired center frequency, FBW and notch frequency are given, the parameters (l_1, l_2, l_3, l_4, w_1, w_2, w_3, and w_4) of DCSR can be determined according to the design formulas and figures; DCSR is coupled with PCTL. A basic wideband BPF with fixed FWB andnotch is thus presented with fixed C_1, C_2, and C_3;
2) When suitable voltages V_1, $V_{2,}$ and V_3 are set, the simultaneous bandwidth and notch tuning can be achieved by the variable capacitance C_1, C_2, and C_3.

IV. SIMULATED AND MEASURED RESULTS

Subsequently, based on the above analysis and plots, a wideband BPF at 6 GHz with simultaneous bandwidth and notch tuning is designed. The photograph of the prototype is shown in Fig. 9 and the size is 27.4 mm × 12.7 mm. The dimensions are given as: $l_1 = 8.0$ mm, $l_2 = 4.0$ mm, $l_3 = 1.8$ mm, $l_4 = 1.5$ mm, $w_1 = 0.2$ mm, $s = 0.2$ mm, $g = 0.2$ mm, $w_2 = 0.4$ mm, $w_3 = 0.4$ mm, $w_4 = 0.5$ mm, $C_{b1} = 1.2$ pF, $C_{b2} = 4.0$ pF, and the radius of the via holes are 0.2 to 0.3 mm. By applying different voltages, the bandwidth and

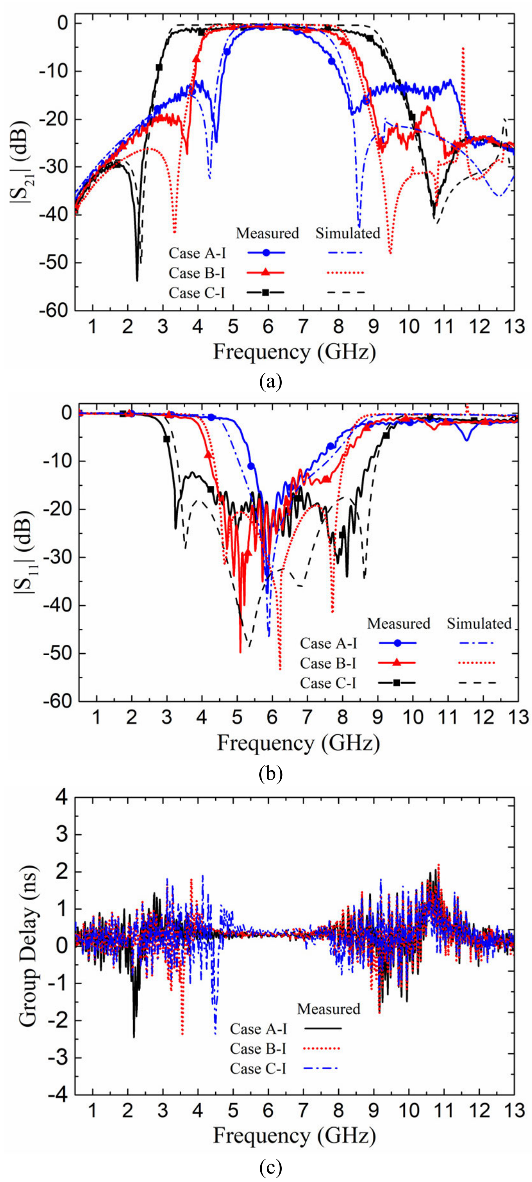

FIGURE 10. Simulated and measured (a) $|S_{21}|$; (b) $|S_{11}|$ and (c) group delay of the proposed BPF with Function-I when $V_1 = 0$, V_2 and V_3 are varied. (Case A-I: $V_2 = -25$ V, $V_3 = -1$ V; Case B-I: $V_2 = -14$ V, $V_3 = -10$ V; Case C-I: $V_2 = -5$ V, $V_3 = -25$ V).

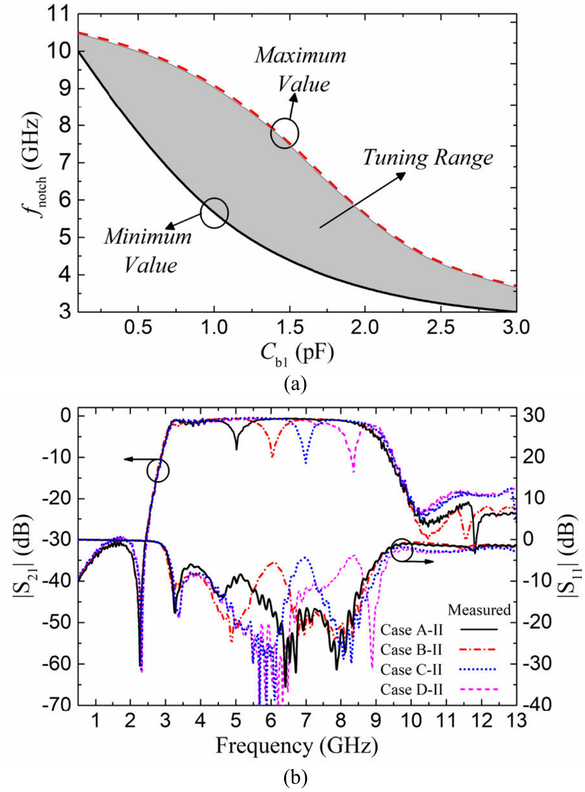

FIGURE 11. (a) Tuning range of notch versus C_{b1}; (b)measured results of the proposed BPF with Function-II when $V_2 = -5$ V, $V_3 = -25$ V are fixed and V_1 is varied. (Case A-II: $C_1 = -1$ V; Case B-II: $V_1 = -10$ V; Case C-II:$V_1 = -20$ V; Case D-II: $V_1 = -25$ V).

notch can be tuned independently. Three tuning functions of the proposed wideband BPF are summarized as follows.

A. FUNCTION I – TUNABLE BANDWIDTH WITHOUT NOTCH IN-BAND

As discussed in Section III, when the capacitance of C_1 decreases to 0, f_{notch} moves out of the upper passband and at a very high frequency. Therefore, when $V_1 = 0$ V, only V_2 and V_3 are applied with different voltages, the proposed BPF with a tunable bandwidth and without notch in-band is achieved. The simulated and measured results with three tuned cases are plotted in Fig. 10. It can be seen that the lower passband edge can be tuned from 3.1 to 5.0 GHz when V_2 is applied with the voltages of −5, −14 and −25 V, while the upper side is tuned from 7.2 to 8.9 GHz when V_3 is applied with –1, –10 and −25 V. The two passband edges can be controlled simultaneously according to Section III. Therefore, the 3-dB passband bandwidth can be tuned from 2.5 to 5.8 GHz with FBW is varied from 41.7% to 96.7%, and there is no notch in the passband. Besides, the measured insertion loss is less than 2.2 dB, the measured return loss is better than 12 dB and the group delay is less than 2.5 ns.

B. FUNCTION II – TUNABLE NOTCH WHEN BANDWIDTH IS KEPT UNCHANGED

The proposed wideband BPF can also realize the function of the tunable notch with constant absolute bandwidth. According to Fig. 7(c), the notch frequency can be varied over the whole passband theoretically. However, the bias circuit and the block capacitor C_{b1} in the practical circuit will lead the measured frequencies and tunable range of notch are slightly different from the simulations. The tuning range of the notch versus C_{b1} is plotted in Fig. 11(a), where a maximum tuning range can be achieved for $C_{b1} = 1.2$ pF. When $V_2 = -5$ V, $V_3 = -25$ V are fixed, and V_1 is applied with –1, −10, −20 and −25 V. The measured results with four tuned cases are recorded in Fig. 11(b). As illustrated, the 3-dB passband is from 3.0 to 8.9 GHz with 98.3% FBW at a center frequency of 6.0 GHz. A tunable notch varies from 5.0 to 8.2 GHz with a 3.2 GHz tuning range with more than 10 dB attenuation.

TABLE 1. Summary of simulated and measured results.

Designed Functions		Center Frequency (GHz)	Bandwidth (GHz) Case A (Minimum BW)	Case B (Medium BW)	Case C (Maximum BW)	Notch Frequency (GHz)
Function-I	Simulated	6.0	4.9-7.6 (2.7)	4.0-8.2 (4.2)	3.0-9.0 (6.0)	Out of Passband
	Measured	**6.0-6.1**	**4.8-7.3(2.5)**	**4.1-8.1 (4.0)**	**3.1-8.9 (5.8)**	
Function-II	**Measured**	**6.0**	**Fixed from 3.1-8.9 (5.8)**			**Tuned From 5.0-8.2 (3.2)**
Function-III	Simulated	6.0-6.1	4.5-7.4 (2.9)	4.0-8.4 (4.4)	3.0-9.2 (6.2)	Fixed at 5.9
	Measured	**5.9-6.1**	**4.6-7.2 (2.6)**	**4.0-8.2 (4.2)**	**3.1-9.1 (6.0)**	**Fixed at 5.9**

TABLE 2. Comparison between this design and previous works.

Designs	Center Frequency (GHz)	Numbers of Tuning Elements	Numbers of Poles	Numbers of Zeros	ABW Tuning Range (GHz)	FBW Tuning Range (%)	Notch Tuning Range (GHz)
[7]	1.9	4	2	0	0.31-0.67 (0.36)	16.3-35 (19.7)	×
[8]	2.0	20	5	0	0.51-0.97 (0.46)	26-49.8 (23.8)	×
[9]	1.0	6	2	0	0.065-0.18 (0.115)	6.5-18 (11.5)	×
[21]	5.7	4	3	2	1.98-3.2 (1.22)	34.8-56.5 (21.7)	×
[13]	6.8	16	–	–	×	×	5.1-5.55 (0.45)
[18]	6.8	3	4	3	×	×	4.6-6.5 (1.9)
This Work	**6.0**	**3**	**6**	**3**	**2.5-5.8 (3.3)**	**41.7-96.7 (55)**	**5.0- 8.2 (3.2)**

Moreover, the insertion loss is lower than 2.6 dB. Group delay is less than 2.8 ns and the return loss is better than 10 dB.

C. FUNCTION III – TUNABLE BANDWIDTH WITH A FIXED NOTCH IN-BAND

Similar to Function-I, if V_1 is applied with a fixed voltage of -10 V, while V_2 is applied with -5, -14 and -25 pF and V_3 is applied with -1, -10 and -25 V, the proposed wideband BPF with a tunable bandwidth and a fixed notch f_{notch} in the passband is thus achieved. As shown in Fig. 12, the measured result exhibits that similar observation can be found for the 3-dB passband bandwidth, which can be tuned from 2.6 to 6.0 GHz with 3.4 GHz tuning range, a fixed notch is at 5.9 GHz with more than 13 dB attenuation. The measured minimum insertion loss is 2.3 dB. Due to the parasitic loss and soldering errors in practical circuit, the insertion loss of the measured results is worse near the higher passband edge. In addition, the return loss is better than 10 dB and the group delay is less than 2.8 ns. The measured and simulated results of Function I, II and III are summarized in Table 1.

A comparison of this design with some previous works is summarized in Table 2. It can be seen that only the proposed wideband BPF with maximum numbers of poles can control both the bandwidth and notch, and it has the widest absolute bandwidth (ABW) tuning range, which is 3.2 GHz. It can also realize a tunable notch from 5.0 to 8.2 GHz with a 3.2 GHz tuning range. The bandwidth and notch can be tuned simultaneously. In addition, this new design requires the least number of tuning elements for similar ABW tuning ranges like [6] and [18]. Due to its simple structure and good performance, the proposed tunable BPF is attractive for both tunable elements and wideband communication applications.

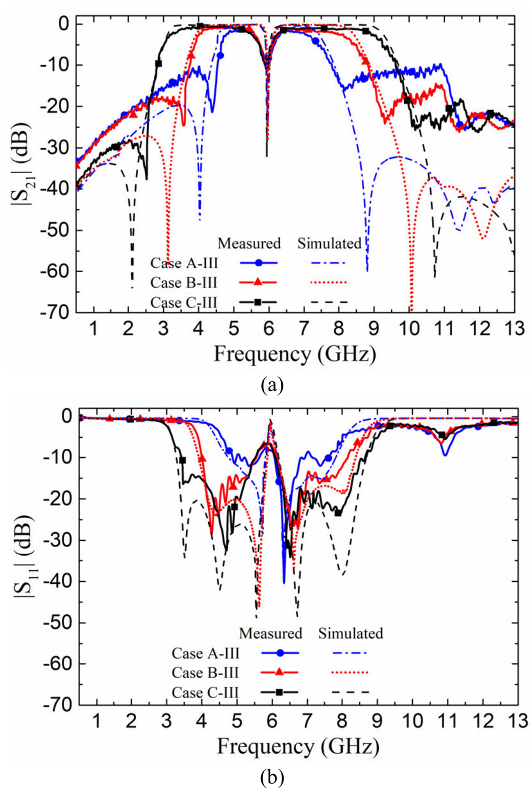

FIGURE 12. Simulated and measured (a) $|S_{21}|$ and (b) $|S_{11}|$ of the proposed BPF with Function-III when $V_1 = -10$ V, C_2 and C_3 are varied. (Case A-I: $V_2 = -25$ V, $V_3 = -1$ V; Case B-I: $V_2 = -14$ V, $V_3 = -10$ V; Case CI: $V_2 = -5$ V, $V_3 = -25$ V).

V. CONCLUSION

A wideband BPF integrated the functions of simultaneous bandwidth and notch tuning based on a novel DCSR and PCTL, is presented. The bandwidth tuning is approximated by the passband edges zeros and poles control because the cutoff frequencies are bounded by the passband edge zeros and poles. The PCTL provides two additional poles to widen the passband and two zeros in the stopband to improve the sharpness of the passband edges. The bandwidth and the notch frequency can be tuned independently and simultaneously by three lumped varactors. The prototype reports that when center frequency is at 6 GHz, the ABW has 3.3 GHz tuning range with 55% FBW tuning. Furthermore, the notch tuning range is 3.2 GHz. The DCSR structure is attractive in the design of tunable wideband BPFs.

REFERENCES

[1] A. Brown and G. Rebeiz, "A varactor-tuned RF filter," *IEEE Trans. Microw. Theory Techn.*, vol. 48, no. 7, pp. 1157–1160, Jul. 2000.
[2] C. Lugo and J. Papapolymerou, "Dual-mode reconfigurable filter with asymmetrical transmission zeros and center frequency control," *IEEE Microw. Wireless Compon. Lett.*, vol. 16, no. 9, pp. 499–501, Sep. 2006.
[3] W. Tang and J.-S. Hong, "Varactor-tuned dual-mode bandpass filters," *IEEE Trans. Microw. Theory Techn.*, vol. 58, no. 8, pp. 2213–2219, Aug. 2010.
[4] C. Lugo and J. Papapolymerou, "Six-state reconfigurable filter structure for antenna based systems," *IEEE Trans. Antennas Propag.*, vol. 54, no. 2, pp. 479–483, Feb. 2006.
[5] Y.-H. Chun and J.-S. Hong, "Electronically reconfigurable dual-mode microstrip open-loop resonator filter," *IEEE Microw. Wireless Compon. Lett.*, vol. 18, no. 7, pp. 449–451, Jul. 2008.
[6] Z. Zhao, "Comments on 'A quasi elliptic function 1.75–2.25 GHz 3-pole bandpass filter with bandwidth control'," *IEEE Trans. Microw. Theory Techn.*, vol. 62, no. 11, p. 2843, Nov. 2014.
[7] W.-H. Tu, "Compact low-loss reconfigurable bandpass filter with switchable bandwidth," *IEEE Microw. Wireless Compon. Lett.*, vol. 20, no. 4, pp. 208–210, Apr. 2010.
[8] A. Miller and J.-S. Hong, "Wideband bandpass filter with reconfigurable bandwidth," *IEEE Microw. Wireless Compon. Lett.*, vol. 20, no. 1, pp. 28–30, Jan. 2010.
[9] G. Zhang, Y. Xu, and X. Wang, "Compact tunable bandpass filter with wide tuning range of centre frequency and bandwidth using short coupled lines," *IEEE Access*, vol. 6, pp. 2962–2969, 2018.
[10] S. W. Wong and L. Zhu, "Implementation of compact UWB bandpass filter with a notch-band," *IEEE Microw. Wireless Compon. Lett.*, vol. 18, no. 1, pp. 10–12, Jan. 2008.
[11] H. Shaman and J.-S. Hong, "Ultra-wideband (UWB) bandpass filter with embedded band notch structure," *IEEE Microw. Wireless Compon. Lett.*, vol. 17, no. 3, pp. 193–195, Mar. 2007.
[12] J. Xu, W. Wu, W. Kang, and C. Miao, "Compact UWB bandpass filter with a notched band using radial stub loaded resonator," *IEEE Microw. Wireless Compon. Lett.*, vol. 22, no. 7, pp. 351–353, Jul. 2012.
[13] L. Kurra, M. P. Abegaonkar, A. Basu, and S. K. Koul, "Switchable and tunable notch in ultra-wideband filter using electromagnetic bandgap structure," *IEEE Microw. Wireless Compon. Lett.*, vol. 24, no. 12, pp. 839–841, Dec. 2014.
[14] L. Zhu, S. Sun, and W. Menzel, "Ultra-wideband (UWB) bandpass filters using multiple-mode resonator," *IEEE Microw. Wireless Compon. Lett.*, vol. 15, no. 11, pp. 796–798, Nov. 2005.
[15] M. Makimoto and S. Yamashita, "Bandpass filters using parallel coupled stripline stepped impedance resonators," *IEEE Trans. Microw. Theory Techn.*, vol. 28, no. 12, pp. 1413–1417, Dec. 1980.
[16] Y.-C. Chiou, J.-T. Kuo, and E. Cheng, "Broadband quasi-Chebyshev bandpass filters with multimode stepped-impedance resonators (SIRs)," *IEEE Trans. Microw. Theory Techn.*, vol. 54, no. 8, pp. 3352–3358, Aug. 2006.
[17] C. H. Kim and K. Chang, "Ring resonator bandpass filter with switchable bandwidth using stepped-impedance stubs," *IEEE Trans. Microw. Theory Techn.*, vol. 58, no. 12, pp. 3936–3944, Dec. 2010.
[18] H. Wang, K.-W. Tam, S.-K. Ho, W. Kang, and W. Wu, "Design of ultra-wideband bandpass filters with fixed and reconfigurable notch bands using terminated cross-shaped resonators," *IEEE Trans. Microw. Theory Techn.*, vol. 62, no. 2, pp. 252–265, Feb. 2014.
[19] J.-R. Mao, W.-W. Choi, K.-W. Tam, W. Q. Che, and Q. Xue, "Tunable bandpass filter design based on external quality factor tuning and multiple mode resonators for wideband applications," *IEEE Trans. Microw. Theory Techn.*, vol. 61, no. 7, pp. 2574–2584, Jul. 2013.
[20] T. Cheng and K.-W. Tam, "A wideband bandpass filter with reconfigurable bandwidth based on cross-shaped resonator," *IEEE Microw. Wireless Compon. Lett.*, vol. 27, no. 10, pp. 909–911, Oct. 2017.
[21] X.-K. Bi, T. Cheng, P. Cheong, S.-K. Ho, and K.-W. Tam, "Design of dual-band bandpass filters with fixed and reconfigurable bandwidths based on terminated cross-shaped resonators," *IEEE Trans. Circuits Syst., II, Exp. Briefs*, vol. 66, no. 3, pp. 317–321, Mar. 2019.
[22] P. Cheong, S.-W. Fok, and K.-W. Tam, "Miniaturized parallel coupled-line bandpass filter with spurious-response suppression," *IEEE Trans. Microw. Theory Techn.*, vol. 53, no. 5, pp. 1810–1816, May 2005.
[23] S.-W. Ting, K.-W. Tam, and R. Martins, "Miniaturized microstrip lowpass filter with wide stopband using double equilateral U-shaped defected ground structure," *IEEE Microw. Wireless Compon. Lett.*, vol. 16, no. 5, pp. 240–242, May 2006.
[24] S. Yamamoto, T. Azakami, and K. Itakura, "Coupled strip transmission line with three center conductors," *IEEE Trans. Microw. Theory Techn.*, vol. 14, no. 10, pp. 446–461, Oct. 1966.

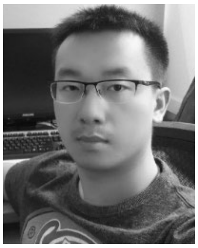

CHENG TENG (Student Member, IEEE) was born in Hunan, China, in 1991. He received the B.Sc. and M.Sc. degrees in electrical and computer engineering from the University of Macau, Macau, China, in 2013 and 2016, respectively, where he is currently pursuing the Ph.D. degree.

Since November 2013, he has been a Research Assistant with the Wireless Communication Laboratory, Faculty of Science and Technology, University of Macau. His researches focus on the UWB bandpass filters, tunable bandpass filters, differential bandpass filters, and RFID systems.

PEDRO CHEONG (Member, IEEE) received the Ph.D. degree in electrical and electronics engineering from the University of Macau, Macau, in 2014.

In 2005, he joined the Wireless Communication Laboratory, University of Macau, as a Research Fellow, and he was a Laboratory Affairs Officer in 2008. He is currently a Lecturer (UM Macao Fellow) with the Department of Electrical and Computer Engineering. Meanwhile, he is also a Visiting Research Fellow with the Poly-Grames Research Center, Ecole Polytechnique (University of Montreal), Canada. He has published over 35 peer-reviewed articles in top tier journals and international conferences. His research interests include RF/MW passive filter designs, circuit modeling, antenna arrays, RFID systems, multiband communication, and advanced wireless transceiver systems.

Dr. Cheong was a member of the organizing committee of the 2010 International Symposium on Antennas and Propagation. He received the Macao Science and Technology Award for Postgraduates, in 2012, and two best student paper awards in different international conferences. Since 2015, he has been serves as the secretary of the IEEE Macau AP/MTT Joint Chapter. He is a Reviewer of the IEEE Transactions on Microwave Theory and Techniques, the IEEE Microwave and Wireless Components Letters, IEEE Access, *IET Microwaves, Antennas and Propagation*, and the *Journal of Electromagnetic Waves and Applications*.

SUT-KAM HO was born in Macau, China, in 1974. She received the B.Eng. degree in electrical and electronics engineering from the University of Macau, Taipa, Macau, in 1995, the B.Sc. and M.Phil. degrees in physics from The Hong Kong University of Science and Technology, Hong Kong, in 1997 and 1999, respectively, and the Ph.D. degree in physics from Hong Kong Baptist University, Hong Kong, in 2007. Since 2007, she has been an Assistant Professor with the Faculty of Science and Technology, University of Macau. Her research interests include laser material interaction, spectroscopy, and trace analysis. She pioneered an analytical technique of plume laser-excited atomic fluorescence, which is capable of highly sensitive elemental analysis and successfully applied this tool for the analysis of aqueous and solid samples. Moreover, she used laser spectroscopy to analyze gemstones with minimal destruction of samples and organics thin film with high-resolution depth profiling. Dr. Ho is a member of the Society of Applied Spectroscopy (U.S.). She is an Active Member of a few local science promotion programs.

KAM-WENG TAM (Senior Member, IEEE) received the B.Sc. degree in electrical and electronics engineering from the University of Macau, Taipa, Macau, China, in 1993, and the joint Ph.D. degree in electrical and electronics engineering from the University of Macau and the Instituto Superior Técnico (IST), Technical University of Lisbon, Lisbon, Portugal, in 2000.

From 1993 to 1996, he was with the Instituto de Engenharia de Sistemas e Computadores (INESC), Lisbon, where he participated in research and development on a broad range of applied microwave technologies for satellite communication systems. From July 2000 to December 2001, he was the Director of the Instituto de Engenharia de Sistemas e Computadores (INESC)–Macau. In 2001, he cofounded the microelectronic design house Chipidea Microelectrónica, Macau, where until 2003, he was the General Manager. Since 1996, he has been with the University of Macau, where he is currently a Professor and the Associate Dean (Research and Graduate Studies) of the Faculty of Science and Technology. He has authored or coauthored over 100 journal and conference papers. His research interests have concerned multifunctional microwave circuits, RFID, UWB for material analysis, and terahertz technology.

Dr. Tam was an Interim Secretary for the establishment of the Macau Section, in 2003. He supervised two IEEE Microwave Theory and Techniques Society (IEEEMTT-S) Undergraduate Scholarship recipients, in 2002 and 2003. He was a Founder of the IEEE Macau AP/MTT Joint Chapter in 2010 and was the Chair in 2011–2012. He was a member of the organizing committees of 21 international and local conferences, including the Co-Chair of APMC2008, the Co-Chair of the Technical Program, IEEE MTT-S International Microwave Workshop Series on Art of Miniaturizing RF and Microwave Passive Components, in 2008, and the Co-Chair of ISAP2010.

WAI-WA CHOI (Senior Member, IEEE) was born in Macau, China, in 1970. He received the B.Sc., M.Sc., and Ph.D. degrees in electrical and electronics engineering from the University of Macau, Macau, in 1993, 1997, and 2008, respectively.

From 1993 to 1995, he was with the Institute of Systems and Computer Engineering (INESC), Lisbon, Portugal, as a Research Assistant. Since 1995, he has been with the University of Macau, where he is currently an Associate Professor with the Department of Electrical and Computer Engineering. He has authored or coauthored over 60 internationally refereed journal and conference papers. His research interests are in the areas of microwave active and passive circuits, smart antennas, and RF identification (RFID) systems.

Dr. Choi was the Chair of the IEEE Macau Antennas and Propagation/Microwave Theory and Techniques Joint Chapter, in 2015 and 2016.